International Journal of Greenhouse Gas Control 87 (2019) 89–99

Contents lists available at ScienceDirect

International Journal of Greenhouse Gas Control

journal homepage: www.elsevier.com/locate/ijggc

# Heating load depreciation in the solvent-regeneration step of absorption-based acid gas removal using an ionic liquid with an imidazolium-based cation

Bilal Kazmi[a,1], Junaid Haider[b,1], Muhammad Abdul Qyyum[b], Saad Saeed[c], Mohib Raza Kazmi[a], Moonyong Lee[b,*]

[a] Department of Applied Chemistry and Chemical Technology, University of Karachi, Pakistan
[b] School of Chemical Engineering, Yeungnam University, Gyeongsan, 712–749, Republic of Korea
[c] Department of Chemical Engineering, NFC-Institute of Engineering and Technology, Multan, Pakistan

ARTICLE INFO

*Keywords:*
Acid gas removal
Ionic liquids
Absorption
Solvent regeneration
Thermal energy
Total annualized cost

ABSTRACT

Natural gas is a cleaner energy source compared to other fossil-based energy sources owing to its low emissions. However, natural gas contains acidic gases (including $CO_2$ and $H_2S$), which may cause equipment corrosion and environmental damage. To date, amine-based absorption techniques have been used to remove acidic gases from natural gas to reach regulated concentration limits. However, a tremendous amount of heating is required to regenerate amine-based solvents, which remains a major issue with traditional absorption-based acid gas removal units. In this context, 1-butyl-3-methyimidazolium methyl sulfate (bmim)($CH_3SO_4$) and 1-butyl-3-methylimidazolium hexafluorophosphate (bmim)($PF_6$) were adopted as potential solvents for reducing the heating requirements in the solvent-regeneration step of absorption-based removal techniques. This study shows that by using the imidazolium-based cationic IL, up to 99 wt% of acid gases can be removed while dramatically reducing the heating load and the total annualized cost compared to conventional amine-based absorption units. Flash-based solvent regeneration was used to recover the solvent with a heating loading value of 3978 kW, which is 78.6% lower than that of conventional amine regeneration strippers. Use of only flash column instead of stripper also makes the proposed ionic liquid-based absorption technique most economical with respect to capital investment.

## 1. Introduction

Global warming is a serious issue in present times. Large amount of $CO_2$, which contributes to global warming, is emitted from coal- and oil-based power plants (Qyyum et al., 2018a). Considering the current energy challenges associated with environment, natural gas (NG) has been recognized as a cleaner energy source compared to conventional coal and oil (Qadeer et al., 2018; Qyyum et al., 2019). Therefore, the NG has become one of the most dominant global energy sources (Qyyum et al., 2018b). However, NG contains a certain amount of acid gases such as $CO_2$ and $H_2S$ which deteriorate its cleanliness and desirable thermal properties. Furthermore, the presence of $CO_2$ and $H_2S$ increases the cost of green utilization of NG mainly because of their corrosiveness towards equipment and toxicity.

To date, several approaches including absorption, adsorption, and membrane separation have been developed to capture acid gases from NG. Absorption-based techniques are the most common and practical approaches for large-scale NG treatment to remove acid gases (Afkhamipour and Mofarahi, 2014). Aqueous alkanolamine solvent-based absorption/stripper schemes have been developed for acid gas removal, mainly because of their high reliability. Among alkanolamine solvents, ethanolamine (MEA)-based solvents (e.g., MEA and MDEA) are commonly used because of their strong reactivity, high capacity, active kinetics, and widespread availability with low cost (Lepaumier et al., 2009; Venkatraman and Alsberg, 2017). However, a tremendous amount of thermal energy is required for the regeneration of MEA and MDEA, which accounts for around 80% of the total operating cost (Aaron and Tsouris, 2005; Mesbah et al., 2018). Therefore, the heating load for amine solvent regeneration is a major

* Corresponding author at: Process System Design and Control Laboratory, School of Chemical Engineering Building# 401, Yeungnam University, Dae-dong 214-1, Gyeongsan, 712-749, Republic of Korea.
*E-mail address:* mynlee@yu.ac.kr (M. Lee).
[1] These two authors contributed equally to this work.

https://doi.org/10.1016/j.ijggc.2019.05.007
Received 30 November 2018; Received in revised form 21 April 2019; Accepted 8 May 2019
1750-5836/ © 2019 Elsevier Ltd. All rights reserved.

**Nomenclature**

| | |
|---|---|
| (bmim)($CH_3SO_4$) | 1-Butyl-3-methyimidazolium methyl sulfate |
| (bmim)($PF_6$) | 1-Butyl-3-methylimidazolium hexafluorophosphate |
| (bmim)($BF_4$) | 1-Butyl-3-methylimidazolium tetrafluoroborate |
| (bmim)($Tf_2N$) | 1-Butyl-3-methylimidazolium bis(trifluoromethylsulfonyl)imide |
| ($C_6$mim)(TCM) | 1-Hexyl-3-methylimidazolium tricyanomethanide |
| (emim)(eFAP) | 1-Ethyl-3-methylimidazolium tris(nonafluoroethyl)trifluorophosphate |
| EOS | Equation of state |
| IL | Ionic liquid |
| L/F ratio | Liquid to feed ratio |
| MEA | Ethanolamine |
| MDEA | Methyl-di-ethanol-amine |
| NG | Natural gas |
| NRTL-RK | Nonrandom two liquids-Redlich Kwong |
| PR | Peng-Robinson |
| RTIL | Room temperature ionic liquid |
| SRK | Soave Redlich Kwong |
| TAC | Total annualized cost |
| VLE | Vapor liquid equilibrium |

issue with conventional amine-based absorption techniques. Besides high thermal duty requirements, foaming has also been identified as another issue inherent in amine-based absorption columns.

Ionic liquids (ILs) are generally characterized as salts with very low melting points. Most ILs are liquids at room temperature and are sometimes referred to as room temperature ILs (RTILs). Because of their large volume and lattice flexibility, low entropy changes can be achieved (Zeng et al., 2017). ILs typically consist of a large organic cation and an organic or inorganic anion and have received significant attention in the past few years. They can be used as a substitute for traditional industrial solvents (amines) and have been extensively used as absorbents for gas separation because of relatively low foaming tendency (Privalova et al., 2012; Thaim, 2015) and high thermal stability (Fredlake et al., 2004; Meindersma and De Haan, 2012) leading to significant reductions in thermal load with minimal capital investment. For instance, Taheri et al. (2018) investigated the feasibility of using IL (amim)($Tf_2N$) for $CO_2$, CO, and $H_2$ capture. The authors evaluated the performance of select IL in comparison with methanol. Ma et al. (2017) used Aspen Plus to develop a $CO_2$ capture process using (bmim)($BF_4$) and (bmim)($PF_6$) and concluded that (bmim)($BF_4$) was superior because of its low thermal energy requirement for solvent regeneration. Shiflett et al. (2010) proposed a $CO_2$ capture process using 1-butyl-3-methylimidazolium acetate (bmim)(Ac.) and analyzed the thermal energy and economic savings achieved using IL. Zubeir et al. (2018) proposed novel pressure and temperature swing processes for $CO_2$, CO, and $H_2$ separation using 1-hexyl-3-methylimidazolium tricyanomethanide ($C_6$mim)(TCM). The authors concluded that ($C_6$mim) (TCM) reduced the overall energy consumption by up to 60%. de Riva et al., 2017 used imidazolium-based ILs for post combustion $CO_2$ capture, employing a COSMO-based process simulation approach to incorporate the ILs in the Aspen Plus simulation environment. Liu et al. (2016) proposed a method based on COSMO-RS to select appropriate ILs to remove $CO_2$ from shale gas. The authors used (bmim]($Tf_2N$) as a solvent for absorption-based $CO_2$ capture and reported that the thermal energy required for solvent regeneration was reduced by 66.04%. Most recently, Ma et al. (2018) used the same ILs as Liu et al. (2016) and investigated the $CO_2$ capture performance of (bmim]($Tf_2N$) for use in power plants rather than shale gas. Above mentioned works have designed the IL-based processes mainly for $CO_2$ capture from NG and power plant emission gases to reduce the overall operating costs. However, for the NG processing industry, the removal of acid gases ($CO_2$ and $H_2S$) is essential and $CO_2$ removal is insufficient. To the best of our knowledge, designed processes for acid gas removal from NG using ILs have not been reported to date.

Based on previous studies regarding the solubility of $CO_2$, $H_2S$, and $CH_4$, various classes of ILs have been utilized to study their solvent effects. The potential IL should be chosen based on its structural compatibility, experimental solubility, selectivity of the cation and anion, and most importantly its toxicity. The combination of all the factors listed above must be considered for a prospective IL solvent for the absorption of $CO_2$ and $H_2S$. The cation and anion selection among the vast amount of possible combinations is a key consideration of IL research. The solubility of the acid gas components has been studied in cations like pyridinium (Anderson et al., 2007), pyrrolidinium (Song et al., 2010), phosphonium (Ramdin et al., 2013), imidazolium (Anthony et al., 2005; Cadena et al., 2004), and ammonium (Mattedi et al., 2011) with different anions. Among these ILs, imidazolium-based cations have been studied more extensively and have been reported to perform well with respect to $CO_2$ solubility (Cadena et al., 2004). Further attempts have been made to improve the $CO_2$ solubility of imidazolium by adding functionally philic groups by fluorination of the alkyl chain atoms (ethyl, butyl, and hexyl) to good effect (Lee et al., 2010). The capability of imidazolium cations is due to their ability to form hydrogen bonds with solutes, which is significantly greater than other cations and increases its solvation ability (Kazarian et al., 2000). Increasing the alkyl chain length (ethyl > butyl > hexyl) results in a greater free volume, which can

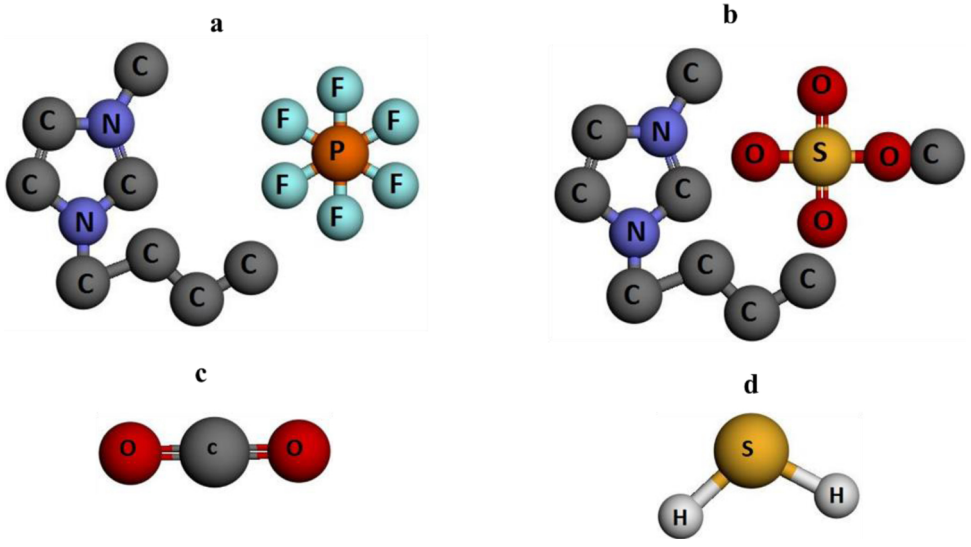


**Fig. 1.** Structural depiction of [bmim][$PF_6$] and [bmim][$CH_3SO_4$].

accommodate more $CO_2$ molecules (Zeng et al., 2017), but also increases IL viscosity (Xiao et al., 2009). Thus, based on the structural aspects of the imidazolium-based butyl chain cations, it is likely that retention would be improved owing to their lower hydrophobicity and comparatively low biodegradability (Ranke et al., 2007).

It has been reported that the overall alkyl chain length and alkyl substitution on ionic liquid cation do not have a significant effect on $CO_2$ solubility and anion seems to dominate the interaction (Wang et al., 2017). In the $PF_6^-$ anion, Phosphorous atom is at center and all the fluorine atoms are arranged in octahedral structure around it as shown in Fig. 1. Due to the high electro negativity of fluorine, all six fluorine atoms having most of the electron density. Pringle et al. (Pringle et al., 2003) also suggested that anion is playing the dominant role in the $CO_2$ absorption. Fluorination on the anion is a common method associated with ionic liquid anions for enhancing the $CO_2$ solubility as compare to the non-fluorinated anions (Raveendran and Wallen*, 2003). Increase in fluorination on the anion enhance the free volume of the IL which contains more $CO_2$ molecules in its voids. In case of $H_2S$ interaction mechanism with IL hydrogen bonding is the dominating force where hydrogen atom act as bond donor and sulfur atom act as bond acceptor as shown in Fig. 1. Sánchez-Badillo et al. (2015) further described the interaction of $H_2S$ with IL using radial distribution function and showed that hydrogen atoms of $H_2S$ are more inclined towards anion part of ionic liquid while cation surrounds the sulfur atom of $H_2S$. $H_2S$ molecule consists of dynamic hydrogen bonding system having smaller dipole moment in comparison to $H_2O$ (i.e. 0.9 and 1.8) and therefore it results in greater solubility in organic solvents. Wang et al. (2017) also observed that $H_2S$ has a rapid rate of solubility in IL generally due to its strong acidic nature and polarity.

Selectivity for $CO_2/H_2S$, $CO_2/CH_4$ and solubility are also important factors while considering structural aspects for the selection of an IL (Table 1) (Jalili et al., 2013). Among the shortlisted candidates, (eFAP)—based anions exhibited high solubility for the absorption of $CO_2$ (Althuluth et al., 2012). ILs with methyl sulfate ($CH_3SO_4$) anions have high polarity and great affinity toward $CO_2$. Selectivity calculated from experimental results shows that $(PF_6)^{--}$based ILs would have the greater solubility (Table 2). In addition, an important factor in cation and anion selection is the availability of experimental data and physiochemical properties of ILs with the relevant components of NG. Therefore, based on these criteria, all possible candidates for acid gas removal are shown in Table 1. Considering the factors stated above, $(PF_6)$– and $(CH_3SO_4)$– with 1-butyl-3-methylimidazolium $(bmim)^+$ cations were selected as the potential ILs for the removal of acid gases from NG. In addition, the toxicity of the IL should be considered as in the study by Liu et al. (Liu et al., 2016) who determined $EC_{50}$ values; higher values indicate less toxic effects on the environment in terms of biodegradability.

In this work, we have sought to investigate the low-viscosity imidazolium cation-based $(bmim)(CH_3SO_4)$ and $(bmim)(PF_6)$ ILs to simultaneously remove $CO_2$ and $H_2S$ from NG. The selected ILs have good thermal stability, low viscosity, high selectivity for acid gases, and lower toxicity than other available ILs as described previously. To analyze the technical and commercial feasibility of the designed process, the Aspen Plus v10 simulator was used for process analysis followed by rigorous regression and experimental validation of the ILs. Rigorous regression of the binary interaction parameters was performed by incorporating the experimental data in ASPEN Plus and the equation of state model of Peng Robinson and SRK (Soave Redlich Kwong) was utilized to calculate the binary interaction parameters. To evaluate the commercial feasibility of the proposed process, the amine-based acid gas removal process was also modeled for economic comparison with the proposed IL-based process. Finally, detailed technical sensitivity analyses and process optimization corresponding to minimal total annualized cost (TAC) were performed.

## 2. Proposed process: Regression, simulation, and description

The basic approach used for designing the $H_2S$ and $CO_2$ removal process from the NG stream using ILs is shown in Fig. 2. The modeling

**Table 1**
Solubility of ILs for acid gas removal.

| Ionic liquid | Solubility of $H_2S$ and $CO_2$ | Conditions of temp (K) | Conditions of pressure (MPa) | References |
|---|---|---|---|---|
| (emim)(eFAP) | It is very less effective than (omim)$(Tf_2N)$ and (bmim)$(PF_6)$ for the separation of $CO_2$ and $H_2S$ gases from each other in gaseous streams, but more effective for the removal of these two acid gases from natural gas. | 303-353 | up to 6 | (Kumełan et al., 2006; Privalova et al., 2012) |
| (bmim)$(PF_6)$ (omim)$(PF_6)$ | It shows that solubility of both gases increases by increasing the number of carbon atom of the alkyl substituent of the methylimidazolium cation ring and increasing the fluorination on anions would increase the ability of IL for removal of gases. | 283.15-403.15 | Up to 14.639 | (Á lvaro Pé rez-Salado Kamps et al., 2003; Hossein Jalili et al., 2009; Jalili et al., 2013; Kumełan et al., 2006) |
| (bmim)$(Tf_2N)$ (omim)$(Tf_2N)$ | It has been concluded that the solubility of $CO_2$ is greater in ILs with anions having − $CF_3$ groups such as $(Tf_2N)$ − and also that the solubility increases by increasing the alkyl group chain. | 303-353 | up to 9 | (Ramdin et al., 2013) |
| (HOemim)$(BF_4)$, (HOemim)$(Tf_2N)$, (HOemim)$(PF_6)$ | solubility of hydrogen sulfide in (HOemim)-based ILs, especially in (HOemim)$(BF_4)$ and (HOemim)$(PF_6)$, is much greater than that of carbon dioxide, indicating that these ILs are efficient solvents for separation of $H_2S$ from $CO_2$. | 303-353 | up to 7 | (Safavi et al., 2013) |
| (bmim)$(CH_3SO_4)$ | The choice of (bmim)$(CH_3SO_4)$ led to a significant increase in the $CO_2/H_2S$ selectivity compared with (bmim)$(PF_6)$. | 295.8-315.4 | up to 9.805 | (Kumełan et al., 2006; Lynnette A. Blanchard et al., 2001; Shiflett et al., 2010) |

**Table 2**
Selectivity for $CO_2$ and $H_2S$ of ILs.

| Ionic liquid | Name | Selectivity ($CO_2/CH_4$) | Toxicity $EC_{50}$ | Selectivity ($CO_2/H_2S$) |
|---|---|---|---|---|
| (bmim)($PF_6$) | 1-butyl-3-methylimidazolium hexafluorophosphate | 38.24 | 2.15 | 1.2-3.7 |
| (bmim)($TF_2N$) | 1-butyl-3-methylimidazolium bis(trifluoromethylsulfonyl)imide | 20.98 | 3.41 | 3.03 |
| (bmim)($CH_3SO_4$) | 1-butyl-3-methylimidazolium methyl sulfate | 35.00 | 3.21 | 7.4-12.4 |
| (emim)(eFAP) | 1-ethyl-3-methylimidazolium tris(nonafluoroethyl)trifluorophosphate | 11.58 | NA | 1.9-1.50 |
| (bmim)($BF_4$) | 1-butyl-3-methylimidazolium tetrafluoroborate | 11.86 | 3.3 | NA |

*All values of selectivity are taken from reference (Wang et al., 2017), NA = not available.

process of ILs using process simulators is complicated. Firstly, ILs are not conventionally included in the databases of the available commercial simulators such as Aspen Plus, Hysys, UniSim, and Pro-II. Secondly, regression of the binary interaction parameters using thermodynamic models in property modeling is severely limited by the lack of experimental data. Therefore, calculation of these parameters using equilibrium data of ILs was performed and was determined using a rigorous regression system.

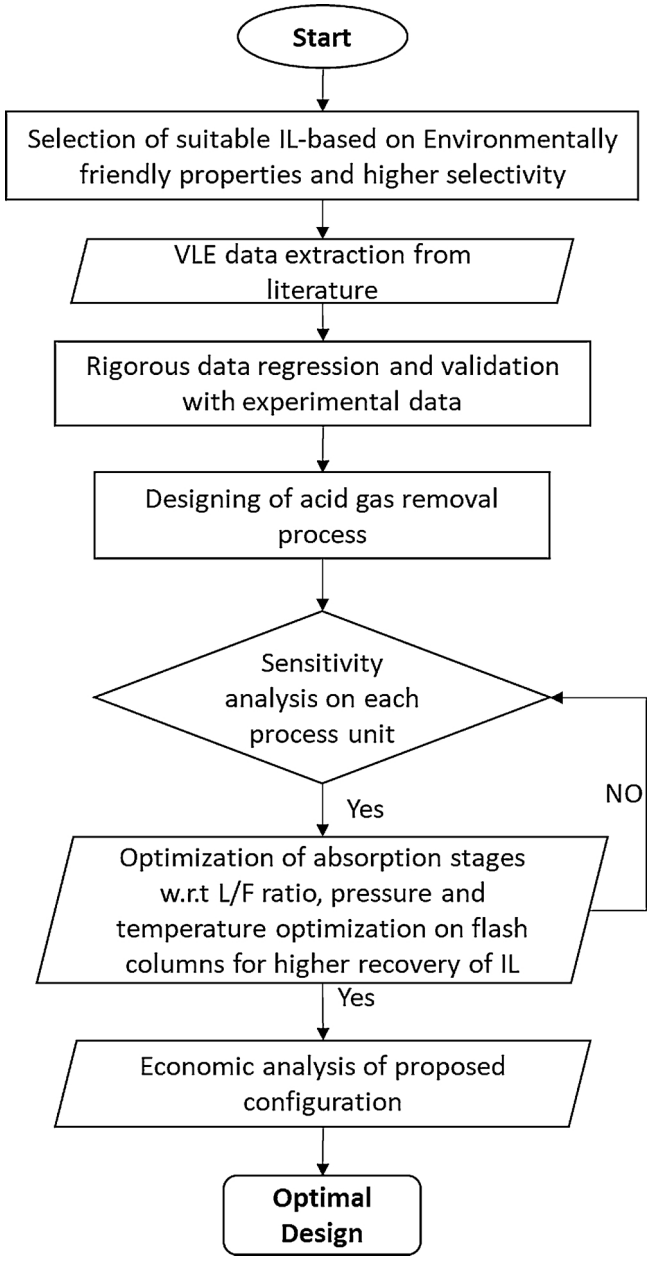


**Fig. 2.** Systematic approach towards optimizing the final design.

Fig. 3 shows the estimated solubility of $CO_2$, $H_2S$, and $CH_4$ in (bmim)($CH_3SO_4$) and (bmim)($PF_6$) as a function of the experimental and estimated pressure. The predictions are in good agreement with the experimental data (reported by different investigations, as given in Table 1) used to develop the thermodynamic models. It is clear that (bmim)($PF_6$) is a better candidate for the removal of the acid gas, while absorbing a smaller amount of $CH_4$.

### 2.1. Thermodynamic model

The Soave-Redlich-Kwong (SRK) and Peng Robinson (PR) state equations form the basis of the process model used as the calculating procedure for determining binary interactions between the ILs (bmim)($CH_3SO_4$) and (bmim)($PF_6$) and $CH_4$, $CO_2$, and $H_2S$. However, the SRK differs from the PR equation as follows:

- The concept of molar volume proposed by Peneloux and Rauzy was further enhanced to increase the liquid volume translation equation from the cubic equation of state.
- Computational response for the SRK equation was enhanced using independent compositional fugacity.
- Phase equilibrium was improved over mixing rules using the method proposed by Kabadi-Danner to improve water-hydrocarbon system calculations.

The standard PR and SRK thermodynamic equations originate from the equation of state (EOS) with the standard alpha function, which has also been used for gas processing, refineries, petrochemical processes, and other related applications. These EOS models may be used with hydrocarbon components including $H_2S$, $CO_2$, and $N_2$. The Physical Property System of Aspen has default (kij) values for a many organic components and pairs. These parameters were utilized in conjunction with the PR and SRK property method. The parameters in the databank differed from those used with other models and this can produce different results. To obtain better results, the binary parameter (kij) must be determined from a regression of the phase equilibrium using experimental vapor liquid equilibrium (VLE) data.

The form of the EOS for the thermodynamic model is:

$$\mathbf{p} = \frac{\boldsymbol{RT}}{\boldsymbol{V_M - b}} - \frac{\boldsymbol{a}}{\boldsymbol{V_m(V_m + b)}} \tag{1}$$

where:

$$\boldsymbol{a = a_0 + a_1} \tag{2}$$

For SRK and Peng-Robinson:

$a_0$ is the standard quadratic mixing term and $a_1$ is an additional, asymmetric (polar) term where

$$\boldsymbol{a_o} = \sum_{i=1}^{n}\sum_{j=1}^{n} \boldsymbol{x_i x_j \sqrt{a_i a_j}(1 - k_{ij})} \tag{3}$$

$$\boldsymbol{a_1} = \sum_{i=1}^{n} \boldsymbol{x_i}\left(\sum_{j=1}^{n} \boldsymbol{x_j}\left(\left((a_i a_j)^{\frac{1}{2}} \boldsymbol{l_{j,i}}\right)^{\frac{1}{3}}\right)\right)^3 \tag{4}$$

$$\boldsymbol{b} = \sum_i \boldsymbol{x_i b_i} \tag{5}$$

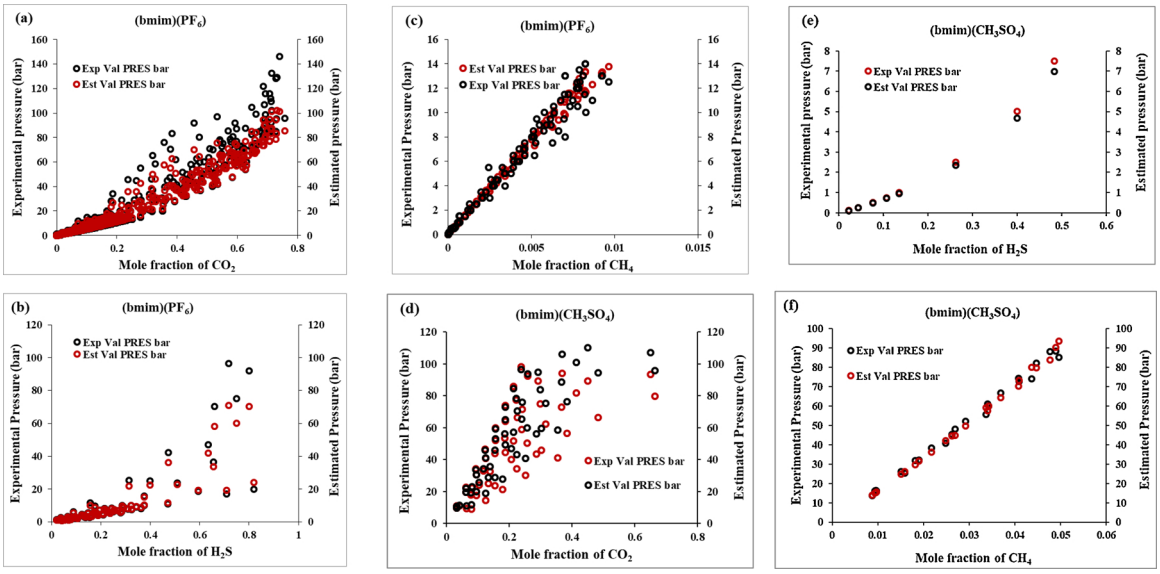


**Fig. 3.** Solubility of acid gases and methane in ILs based on experimental and estimated values. **(a)** Absorption of $CO_2$ in (bmim)($PF_6$); **(b)** absorption of $H_2S$in (bmim)($PF_6$); **(c)** absorption of $CH_4$ in (bmim)($PF_6$); **(d)** absorption of $CO_2$ in (bmim)($CH_3SO_4$); **(e)** absorption of $H_2S$in (bmim)($CH_3SO_4$); and **(f)** absorption of $CH_4$ in (bmim)($CH_3SO_4$).

**Table 3**
Regression results for (bmim)($PF_6$).

| | PR | | | | RK(Redlich-Kwong) | | | | SRK | | | |
|---|---|---|---|---|---|---|---|---|---|---|---|---|
| (bmim)($PF_6$) | $kA_{ij}$ | $kB_{ij}$ | $kC_{ij}$ | Standard deviation | $kA_{ij}$ | $kB_{ij}$ | $kC_{ij}$ | Standard deviation | $kA_{ij}$ | $kB_{ij}$ | $kC_{ij}$ | Standard deviation |
| (bmim)($PF_6$)/$CH_4$ | 0.6071 | 0 | 0 | 0.0330 | 0.6374 | 0 | 0 | 0.0377 | 0.6357 | 0 | 0 | 0.0377 |
| (bmim)($PF_6$)/$H_2S$ | −0.0731 | 0 | 0 | 0.0202 | −0.0728 | 0 | 0 | 0.0222 | −0.0787 | 0 | 0 | 0.0227 |
| (bmim)($PF_6$)/$CO_2$ | −0.0202 | 0 | 0 | 0.0079 | −0.0258 | 0 | 0 | 0.0088 | −0.0355 | 0 | 0 | 0.0084 |
| $CH_4$/$H_2S$ | 0.0879 | 0 | 0 | 0.0014 | 0.0837 | 0 | 0 | 0.0015 | 0.0886 | 0 | 0 | 0.0013 |
| Average deviation | **0.0157** | | | | **0.0176** | | | | **0.0175** | | | |

$$k_{ij} = k_{ij}^{(1)} + k_{ij}^{(2)}T + k_{ij}^{(3)}/T \quad ; \text{Kij=Kji} \tag{6}$$

### 2.2. Data regression and correlation

Regression is a powerful tool to correlate the experimental data for obtaining binary interaction parameters. The experimental data for (bmim)($PF_6$) and (bmim)($CH_3SO_4$) were correlated, and the results are shown in Tables 3 and 4.

### 2.3. Process simulation

Process simulations help to reduce the experimental work required for the development of new processes and products involving ILs. The operating conditions, equipment sizes, operating and capital costs, performance, and even the feasibility of a process can be analyzed by process simulation.

#### 2.3.1. Traditional amine-based acid gas removal unit (base case)

Various technologies have been adopted at the laboratory and industrial scale to remove acid gas components from NG (Abotaleb et al., 2018; Haghtalab and Shojaeian, 2010). Currently, the most commonly utilized method for NG sweetening is an amine-based process (Stewart and Arnold, 2011). Methods based on alkanolamines such as methyldiethanolamine (MDEA) are used as conventional solvents for removing acid gases (Afkhamipour and Mofarahi, 2014; Muhammad and GadelHak, 2015).

An amine-based process was developed for technical evaluation and comparison with the IL-based acid gas-removal design configurations based on the design methodology shown in Fig. 4 (Abdulrahman and Sebastine, 2013). The feed composition and process constraints are listed in Table 5.

The process consists of an absorber, where a 50% solution of MDEA separates $CH_4$ from the acid gases. The stream from the top of the absorber contains mainly methane but requires further purification to

**Table 4**
Regression-based results for (bmim)($CH_3SO_4$).

| | PR | | | | RK | | | | SRK | | | |
|---|---|---|---|---|---|---|---|---|---|---|---|---|
| (bmim)($CH_3SO_4$) | $kA_{ij}$ | $kB_{ij}$ | $kC_{ij}$ | Standard deviation | $kA_{ij}$ | $kB_{ij}$ | $kC_{ij}$ | Standard deviation | $kA_{ij}$ | $kB_{ij}$ | $kC_{ij}$ | Standard deviation |
| (bmim)($CH_3SO_4$)/$CH_4$ | 0.1966 | 0 | 0 | 0.0701 | 0.1747 | 0 | 0 | 0.0807 | 0.1721 | 0 | 0 | 0.0806 |
| (bmim)($CH_3SO_4$)/$H_2S$ | −0.324 | 0 | 0 | 0.1398 | −0.3472 | 0 | 0 | 0.1510 | −0.3464 | 0 | 0 | 0.1504 |
| (bmim)($CH_3SO_4$)/$CO_2$ | 0.0134 | 0 | 0 | 0.0315 | −0.0106 | 0 | 0 | 0.0381 | −0.0021 | 0 | 0 | 0.0358 |
| $CH_4$/$H_2S$ | 0.0879 | 0 | 0 | 0.0013 | 0.08371 | 0 | 0 | 0.0015 | 0.0885 | 0 | 0 | 0.0013 |
| **Average deviation** | 0.0606 | | | | 0.0678 | | | | 0.0670 | | | |

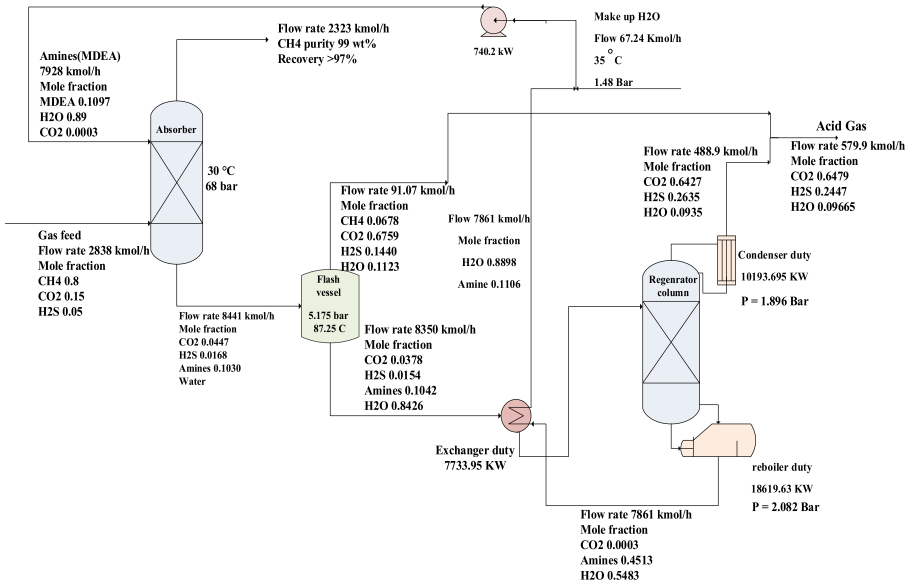


**Fig. 4.** Amine-based process for the removal of acid gases from NG.

satisfy the process constraints (99 wt%). The rich solvent stream from the bottom of the absorber is sent to the flash drum, where the pressure is reduced from 68 to 5.15 bar to remove the remaining impurities in the methane gas together with acid gases. The liquid stream from the bottom flows into the regenerator column, where the amines are regenerated and recycled back into the process. The corresponding process details are listed in Table 6.

However, commercial use of these solutions suffers from certain disadvantages; e.g., a high circulation of amines is required during the process to meet the process specification of > 99% $CH_4$ purity (Sarker, 2016). Amines have a relatively low $CO_2$ loading capacity, causing high pressure in the absorber column (Belmabkhout et al., 2010; McCrellis et al., 2016). In addition, during amine recovery, the regeneration column consumes a large amount of energy for a single process unit compared to the entire amine unit (Mokhatab, 2006).

Other issues associated with this technology occur during the desorption stage where water can leak into the gas stream, affecting its purity. Degradation of the amine is also a serious concern since it results in the formation of organic acids, causing corrosion of the process vessels. Amines are not environmentally friendly because of their volatility (Eide-Haugmo et al., 2009; Hosseinian et al., 2018), necessitating additional steps to overcome these issues. Thus, the introduction of an environmentally friendly and energy-efficient solvent is urgently needed (Øi et al., 2014).

### 2.3.2. IL-based acid gas removal unit

A process was developed to remove the acid gas from NG for further processing following liquefaction. The gas feed enters the bottom of the absorber column which interacts counter-currently with the IL stream entering from the top stage of the absorber. The stream from the top contains the purified NG with while bottom stream is rich in IL. The bottom stream is then moved through the flash columns which are connected in series using the pressure swing phenomena. The IL is regenerated in the flash zone to maintain continuity and the overall process flow diagrams of the IL-based acid gas removal unit are shown in Figs. 5 and 6.

**Table 5**
Feed composition and process constraints for the amine processing unit.

| Feed Composition at 60,000 Kg/h Flow rate<br>Components | Mass Fraction |
|---|---|
| $CH_4$ | 0.80 |
| $CO_2$ | 0.15 |
| $H_2S$ | 0.05 |
| **Feed Conditions** | |
| Temperature (°C) | 30 |
| Pressure (bar) | 68 |
| **Natural gas specification and Constraints** | |
| Recovery (Mass Fractions) | > 0.9 |
| Purity (wt%) | ≥99 |

## 3. Results and discussion

Thermal energy required for the regeneration of the absorbent is the main consideration for process optimization, while the absorber behaves similar to conventional amines. Nevertheless, reducing the thermal load and increasing the absorbent recovery depend on the technology adopted and the properties of the liquid to be regenerated. The major difference in the base case is the regeneration process involves a highly energy intensive distillation operation to obtain high-purity amines for recycling purposes. Furthermore, complete regeneration is complex because of the catch-up of water in the gas stream owing to the requirement of equal proportions of water in

**Table 6**
Process details of the amine-based acid gas removal.

| Process design parameters | |
|---|---|
| **MDEA stream** | |
| Temperature (°C) | 65.53 |
| Pressure (bar) | 83.41 |
| Mole flow (kmol/h) | 7928 |
| Mass Fraction | |
| $H_2O$ | 0.5 |
| MDEA | 0.5 |
| **Absorber** | |
| Stages | 20 |
| Temperature (°C) | 30 |
| Pressure (bar) | 68 |
| $CH_4$ recovery (%) | > 99.5 |
| $CH_4$ purity (%) | 97.5 |
| Make–up water (kmol/h) | 67.42 |
| **Regenerator** | |
| Stages | 18 |
| Reflux ratio (molar) | 1.65 |
| Reboiler duty (kW) | 18611 |
| Pump power for recycling (kW) | 740.2 |

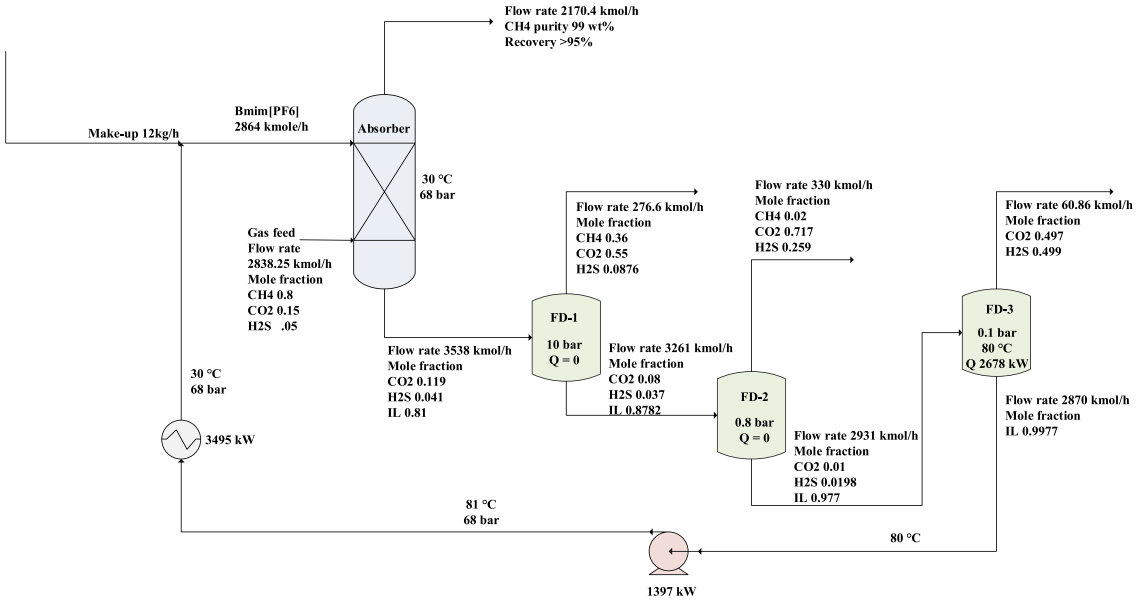


**Fig. 5.** The (bmim)($PF_6$) based acid gas removal unit.

amine-based absorption. Correspondingly, for the IL, recovery is easy because of the low vapor pressure and high boiling point of the IL. The regeneration process only requires flash columns for the easy and complete recovery of IL with very low thermal load (Table 7).

The absorber is the key process unit of the configurations, and its efficiency mainly depends on the liquid flow rate corresponding to the absorption stages. An inverse relation exists between the liquid to feed ratio (L/F) and absorption stages at the required composition. Higher recovery can be achieved by increasing the liquid flow rate, as shown in Fig. 7.

ILs are expensive; therefore, the L/F ratio was optimized for a fixed number of stages (14) and was found to be 1.04 with a > 95% recovery of $CH_4$ for (bmim)($PF_6$) at a column pressure of 68 bar. Similarly for (bmim)($CH_3SO_4$), 13 stages are required for the maximum recovery

**Table 7**
Packed column specifications for (bmim)($CH_3SO_4$) and (bmim)($PF_6$).

| Absorption and Regeneration | (bmim)($CH_3SO_4$) | (bmim)($PF_6$) | MDEA |
|---|---|---|---|
| Absorber stages | 13 | 14 | 20 |
| Absorbent Flow (kmol/h) | 5242 | 2864 | 7928 |
| Make-up flow (kg/h) | – | 3 | 1211 |
| Distillation Column required | – | – | 1 |
| No. of flash drums | 3 | 3 | 1 |
| Column diameter | – | – | 2.44 |
| Stages/trays | 1 | 1 | 18 |
| Regeneration thermal duty (kW) | 3982 | 2678 | 18,619 |
| Pump power (kW) | 2190 | 1397 | 740.2 |

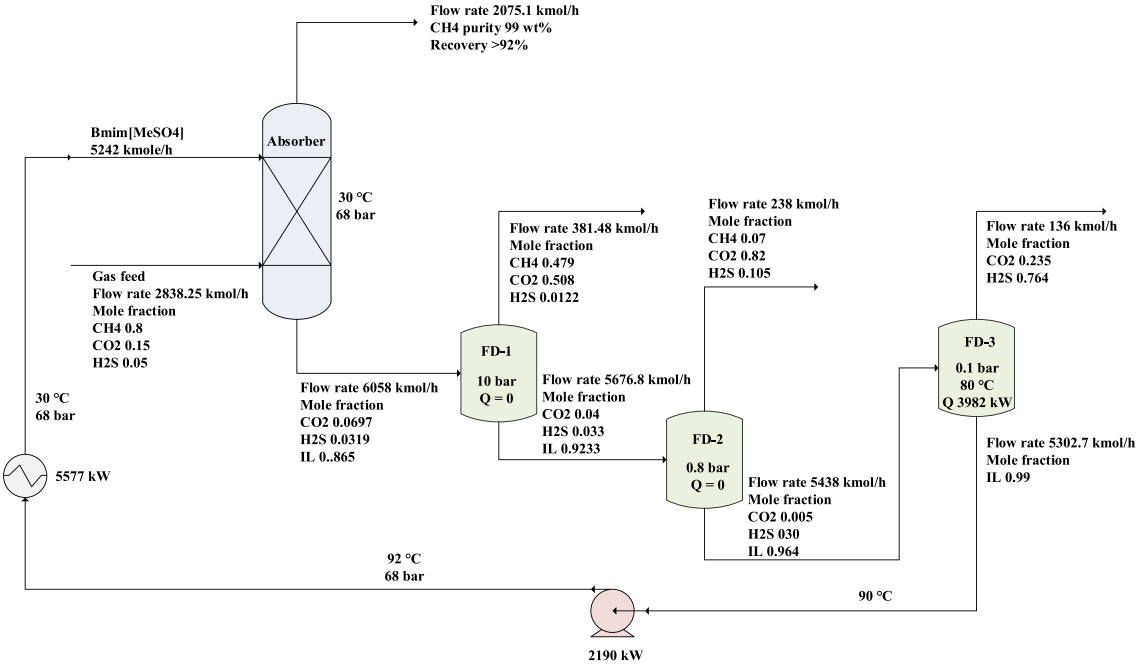


**Fig. 6.** The (bmim)($CH_3SO_4$) based acid gas removal unit.

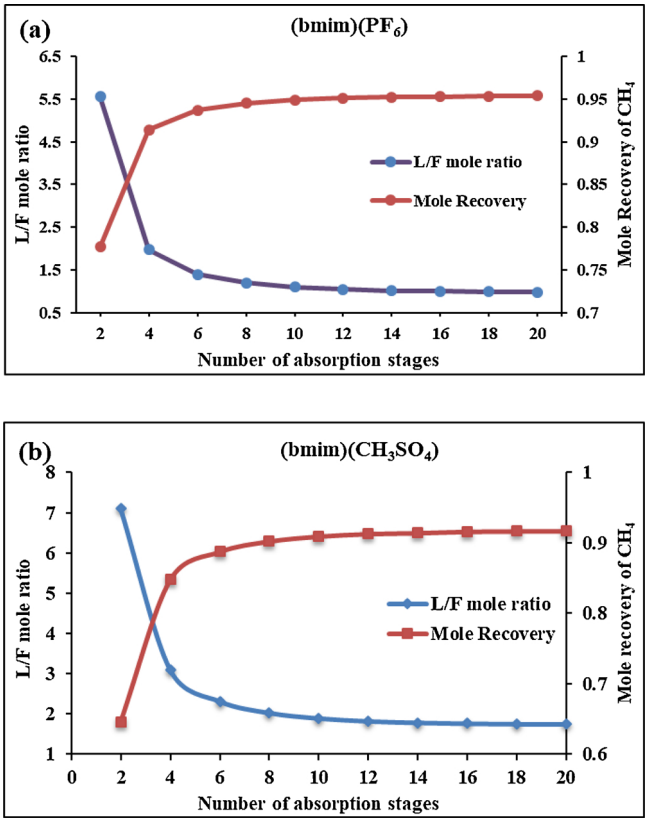


**Fig. 7.** Effect of absorption column stages on the L/F ratio corresponding to methane recovery; (a) (bmim)($PF_6$) and (b) (bmim)($CH_3SO_4$).

(> 92%) of $CH_4$ with an L/F ratio of 1.846. The increased flow rate of (bmim)($CH_3SO_4$) did not affect the separation because of its lower selectivity than (bmim)($PF_6$). Greater than 99% of $CO_2$ was removed from the bottom stream of the absorption column. The solvent stream was allowed to enter the flash drum, where pressure of the IL-rich stream was reduced to 10 bar to recover the remaining methane in the following stream. The IL-stream was then discharged to a second drum for stripping the acid gases from the IL at reduced pressures as low as 0.8 bar. In the final flash drum, the temperature was increased to remove the remaining gas from the IL, which was subsequently recycled back to the absorption column by increasing the pressure to 68 bar.

Sensitivity analysis of the flash drum was performed at various pressures and temperatures to reduce the energy requirements of the system. Fig. 8 shows the effects of pressure on the removal of gases based on the FD-2 liquid stream. Despite the higher boiling range of the IL, under vacuum conditions some contents are lost, which must be considered during process evaluation. However, the flash column is operated at 0.8 bar to maximize the solvent regeneration and most of the gases can be separated. The flash drum was assessed to maximize the removal of gases. It should be noted that some solvent waste is generated using (bmim)($PF_6$), but for (bmim)($CH_3SO_4$), there is no certain solvent loss encountered during the process modelling, as shown in Fig. 8. Since the IL is very expensive, maximum solvent recovery is required.

After passing through the second flash column, most of the IL was recovered, but it still contained acid gas contaminants. Thus, the removal of the acid gas contents is necessary prior to recycling and another flash column was used to completely remove the acid gas. A significant tradeoff exists between product purity and solvent recovery. From Fig. 9(a), when the column operated at 0.1 bar and higher temperatures, some solvent appears in the top stream. Thus, at 70 °C, the solvent in the vapor stream is minimal and almost all gases are removed from the IL with a reboiler thermal load of 2678 kW. According to Fig. 9(b), no waste IL was generated when the column is operated at 0.1 bar. At the elevated temperatures, duty increases rapidly to satisfy the process requirements, i.e., complete removal of the acid gases from the IL stream. At 90 °C, almost complete removal of the acid gas was achieved with a duty of 3981 kW.

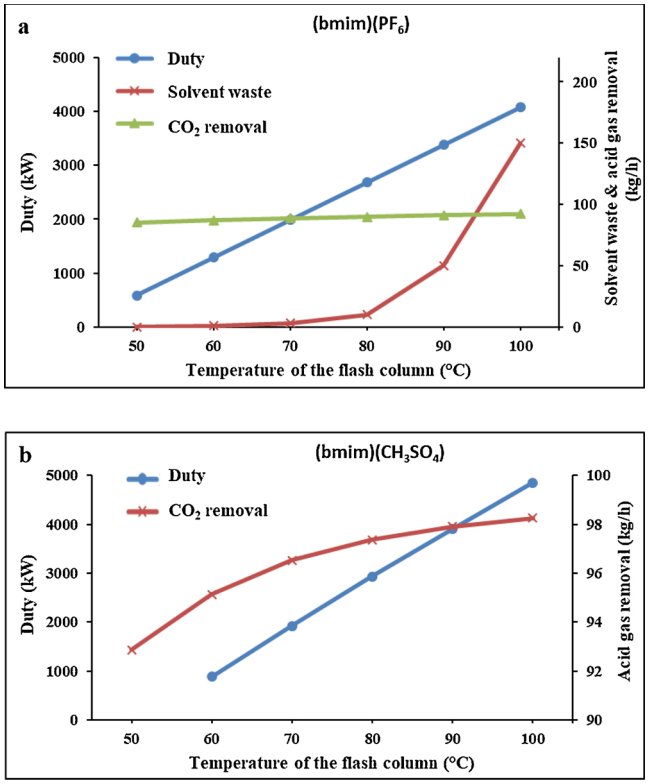


**Fig. 9.** Temperature selection based on minimum reboiler duty corresponding to acid gas removal from the IL; a) (bmim)($PF_6$) and b) (bmim)($CH_3SO_4$).

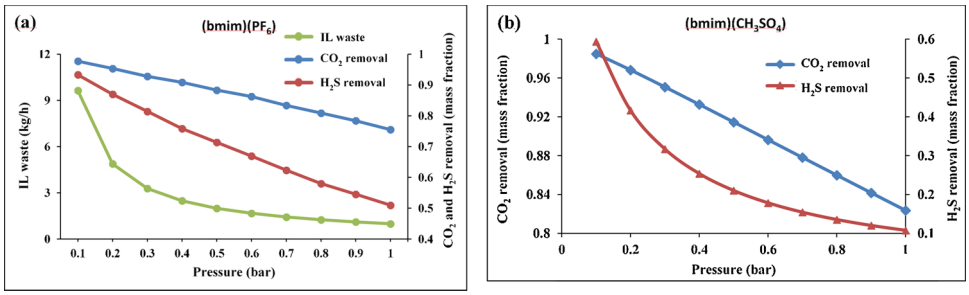


**Fig. 8.** Effect of pressure reduction on acid gas removal; (a) (bmim)($PF_6$) and (b) (bmim)($CH_3SO_4$).

**Table 8**
Comparison between the base case and proposed cases.

| Cost | Amines | (bmim)($PF_6$) | (bmim)($CH_3SO_4$) |
|---|---|---|---|
| Recovery (wt %) | > 95 | > 95 | > 92 |
| Purity (wt %) | 99 | 99.2 | 99 |
| Thermal energy (kW) | 18,619 | 2678 | 3981 |
| Capital cost ($10^6$ $) | 1.42 | 0.938 | 1.125 |
| Operating cost($10^6$ $/y) | 5.319 | 2.442 | 1.95 |
| TAC ($10^6$ $/y) | 5.79 | 2.75 | 2.325 |
| Thermal load savings (%) | – | 85.6 | 78.6 |
| TAC savings (%) | – | 52.5 | 59.8 |

## 4. Technical and economic aspects of the process

Following the process analysis and comparison to the amine unit, the IL showed improved acid gas removal from the NG because the regeneration of the amines is suboptimal. The regeneration requires a large amount of energy and generates a considerable amount of waste. Further, amines alone are unfavorable because of their high viscosity, which can cause corrosion; thus, they must be mixed with water in equal volumes or greater. The regeneration of the amine requires distillation to remove acid gases, corresponding to a reboiler duty of 18,619 kW with minimum of 18 column stages. In addition, consistency of the amine to water ratio and a high make-up of 67.24 kmol/h must be maintained to ensure process continuity. In comparison, ILs can be easily regenerated.

Two flash drums are required to completely regenerate the IL and solvent waste is negligible compared to the amine process. The results show that the ILs are competitive candidates for acid gas removal, reducing energy requirements by up to 3981 kW for (bmim)($CH_3SO_4$) and 2678 kW for (bmim)($PF_6$).

Economic evaluation of each proposed solvent based configuration was performed to evaluate the viability of the proposed processes. All configurations studied were optimized using the process optimization tool in Aspen Plus through a sequential approach based on a sequential quadratic programming (SQP) algorithm to solve nonlinear constrained optimization issues. As described in the process simulation section, the limitations and design goal utilized in the optimization were: (1) NG recovery of > 90 wt%, and (2) NG purity of 99 wt% in the product. The objective function used was the TAC of the proposed configuration. The TAC, which includes both the total energy and equipment purchase (capital) costs, was used to evaluate the economic performance of the proposed configurations. For all process configurations, the TAC was minimized by increasing the number of absorption stages until an optimal number was obtained. Cost relations of the selected equipment based on sizing were obtained from Turton et al., 2008 and cost relations from Zacchello et al. (2018). For a fair comparison, a payback period of 3 years was selected for each configuration, as presented in Eq. (7).

$$TAC = \left(\frac{Capital\ cost}{Payback\ period}\right) + Operating\ cost \tag{7}$$

Table 8 shows the economic comparison of the proposed designs with the base case scenario. The high operating cost of the base case was caused by the high load on the reboiler and high make-up required for amine recirculation, accounting for approximately $\$5.319 \times 10^6$. Alternatively, for the ILs, the pumping cost of the recovered liquids was slightly higher, but the overall cost remained lower than the base case. Consequently, the operating cost using (bmim)($PF_6$) is the sum of the cost of the make-up solvent required on an annual basis and flash duty ($\$2.442 \times 10^6$), which is slightly higher than the (bmim)($CH_3SO_4$) process at $\$1.95 \times 10^6$. Though the TAC of (bmim)($CH_3SO_4$) is lower than that of (bmim)($PF_6$), the latter candidate absorbs acid gases more effectively with high recovery > 95% and purity of the NG product.

Despite the economic feasibility, the key concerns regarding the physical solvents must be considered including the selectivity towards acid gases, viscosity, evaporation rate at higher temperatures, non-corrosivity, and eco-friendliness. The properties of the aforementioned candidates exhibited satisfactory agreement with the desired values.

Hence, the proposed study has presented the acid gas removal from NG using (bmim)($PF_6$) and (bmim)($CH_3SO_4$) with minimal total annualized cost, primarily due to significant heating load depreciation in the solvent-regeneration step. Nevertheless, the $H_2S$ and $CO_2$ are obtained as a mixture which needs further separation considering the practical implementation of the proposed acid-gas removal scheme. In this context, there are several studies carried to propose a process design for the separation of $H_2S$ and $CO_2$ such as pressure swing adsorption (Tomadakis et al., 2011), absorption (Handy et al., 2014), simultaneous separation of $H_2S$ and conversion to elemental sulfur by adsorption using metal-organic framework (Huang and Wang, 2019), etc. The high purity of both $H_2S$ and $CO_2$ gases is mandatory to use them for different profitable industries. For instance, $CO_2$ is used as the main source for the fire extinguishers, carrier to pull out the oil from the well at high pressure in order to enhance the oil recovery, pH controller

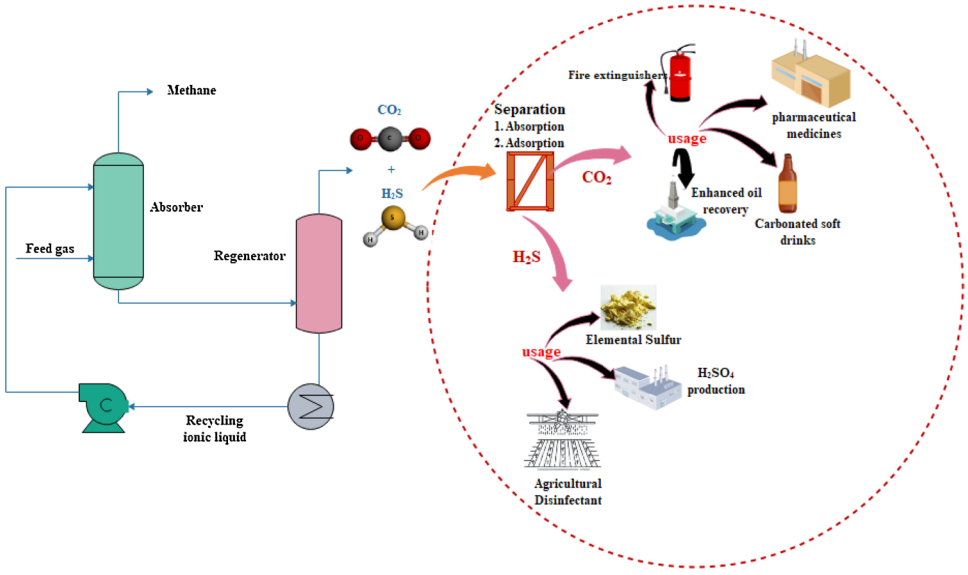


**Fig. 10.** Acid gas removal unit integrated with $H_2S$ and $CO_2$ separation process.

in water treatment process, soldering agent to enhance the metal hardness in metal industry, productive agent in inorganic process industries (in the urea manufacturing). On the contrary, $H_2S$ is used as a main source in the production of $H_2SO_4$ and elemental sulfur. It is also considered as an important component in manufacturing of various inorganic sulfides, pesticides, dyes and in various pharmaceuticals. Hydrogen sulfide is considered as a beneficial reagent for the preparation of reduced sulfur compounds. Some native farmers also utilize $H_2S$ as an agricultural disinfectant. Therefore, as per overall productivity of the system, we are not only making one system sustainable for the environmental conditions but the obtained acid gas ($CO_2$ and $H_2S$) can be a beneficial byproduct which could provide the revenue to the gas processing plant. In this context, the authors would like to extend this study by integrating the acid-gas removal process with $CO_2$ and $H_2S$ separation (see encircled region in Fig. 10) as a future work. The tentative structure of the future work is shown in Fig. 10.

## 5. Conclusions

Imidazolium-cation based ILs (bmim)($CH_3SO_4$) and (bmim)($PF_6$) were examined as potential solvents to remove acid gases from NG to reduce the heating load requirements during solvent regeneration of an absorption-based technique. Using the imidazolium-based cationic ILs, up to 99 wt% of the acid gases can be removed, while dramatically reducing the heating load at minimal total annualized cost compared to conventional amine-based absorption units. The overall thermal energy requirement was reduced by up to 78.6% when compared with amine (MDEA)-based regeneration strippers. Furthermore, the regeneration of the proposed ILs only requires a flash column instead of a stripper, which significantly reduces the total annualized costs.

Further improvement in acid gas absorption may be possible by introducing an ecologically friendly IL with higher selectivity towards acid gases. This could be achieved by studying the toxicity of various ILs and examining their biodegradability. Since ILs are expensive, a blend of amine-based ILs may present a possible solution to balance the excessive costs.

## Declaration

The authors declare no competing financial interest.

## Acknowledgements

This study was supported by the Basic Science Research Program through the National Research Foundation of Korea (NRF) funded by the Ministry of Education (2018R1A2B6001566), and by the Priority Research Centers Program through the National Research Foundation of Korea (NRF) funded by the Ministry of Education (2014R1A6A1031189).

## Appendix A. Supplementary data

Supplementary material related to this article can be found, in the online version, at doi:https://doi.org/10.1016/j.ijggc.2019.05.007.

## References

Ä lvaro Pé rez-Salado Kamps, A., Tuma, D., Xia, J., Maurer, G., 2003. Solubility of CO 2 in the Ionic Liquid. [bmim][PF 6]. https://doi.org/10.1021/je034023f.

Aaron, D., Tsouris, C., 2005. Separation of CO 2 from flue gas: a review. Sep. Sci. Technol. 40, 321–348. https://doi.org/10.1081/SS-200042244.

Abdulrahman, R.K., Sebastine, I.M., 2013. Natural gas sweetening process simulation and optimization: a case study of Khurmala field in Iraqi Kurdistan region. J. Nat. Gas Sci. Eng. 14, 116–120. https://doi.org/10.1016/J.JNGSE.2013.06.005.

Abotaleb, A., El-Naas, M.H., Amhamed, A., 2018. Enhancing gas loading and reducing energy consumption in acid gas removal systems: a simulation study based on real NGL plant data. J. Nat. Gas Sci. Eng. 55, 565–574. https://doi.org/10.1016/J.JNGSE.2017.08.011.

Afkhamipour, M., Mofarahi, M., 2014. Sensitivity analysis of the rate-based CO2 absorber model using amine solutions (MEA, MDEA and AMP) in packed columns. Int. J. Greenh. Gas Control 25, 9–22.

Althuluth, M., Mota-Martinez, M.T., Kroon, M.C., Peters, C.J., 2012. Solubility of carbon dioxide in the ionic liquid 1-ethyl-3-methylimidazolium tris(pentafluoroethyl)trifluorophosphate. J. Chem. Eng. Data 57, 3422–3425. https://doi.org/10.1021/je300521y.

Anderson, J.L., Dixon, J.K., Brennecke, J.F., 2007. Solubility of $CO_2$, $CH_4$, $C_2H_6$, $C_2H_4$, $O_2$, and N 2 in 1-Hexyl-3-methylpyridinium Bis(trifluoromethylsulfonyl)imide: comparison to other ionic liquids. Acc. Chem. Res. 40, 1208–1216. https://doi.org/10.1021/ar7001649.

Anthony, J.L., Anderson, J.L., Maginn, E.J., Brennecke, J.F., 2005. Anion effects on gas solubility in ionic liquids. J. Phys. Chem. B. 109, 6366–6374. https://doi.org/10.1021/jp046404l.

Belmabkhout, Y., Serna-Guerrero, R., Sayari, A., 2010. Adsorption of CO 2 -Containing gas mixtures over amine-bearing pore-expanded MCM-41 silica: application for gas purification. Ind. Eng. Chem. Res. 49, 359–365. https://doi.org/10.1021/ie900837t.

Blanchard, Lynnette A., Zhiyong, Gu, Brennecke*, J.F., 2001. High-Pressure Phase Behavior of Ionic Liquid/CO2 Systems. J. Phys. Chem. B. https://doi.org/10.1021/JP003309D.

Cadena, C., Anthony, J.L., Shah, J.K., Morrow, T.I., Brennecke, J.F., Maginn, E.J., 2004. Why is $CO_2$ so soluble in imidazolium-based ionic liquids? J. Am. Chem. Soc. 126, 5300–5308. https://doi.org/10.1021/ja039615x.

de Riva, J., Suarez-Reyes, J., Moreno, D., Díaz, I., Ferro, V., Palomar, J., 2017. Ionic liquids for post-combustion CO2 capture by physical absorption: thermodynamic, kinetic and process analysis. Int. J. Greenh. Gas Control 61, 61–70. https://doi.org/10.1016/J.IJGGC.2017.03.019.

Eide-Haugmo, I., Brakstad, O.G., Hoff, K.A., Sørheim, K.R., da Silva, E.F., Svendsen, H.F., 2009. Environmental impact of amines. Energy Procedia 1, 1297–1304.

Fredlake, C.P., Crosthwaite, J.M., Hert, D.G., Aki, S.N.V.K., Brennecke, J.F., 2004. Thermophysical properties of imidazolium-based ionic liquids. J. Chem. Eng. Data 49, 954–964.

Haghtalab, A., Shojaeian, A., 2010. Modeling solubility of acid gases in alkanolamines using the nonelectrolyte Wilson-nonrandom factor model. Fluid Phase Equilib. 289, 6–14. https://doi.org/10.1016/J.FLUID.2009.10.005.

Handy, H., Santoso, A., Widodo, A., Palgunadi, J., Soerawidjaja, T.H., Indarto, A., 2014. H2S–CO2Separation using room temperature ionic liquid [BMIM][Br]. Sep. Sci. Technol. https://doi.org/10.1080/01496395.2014.908919.

Hossein Jalili, A., Rahmati-Rostami, M., Ghotbi, C., Hosseini-Jenab, M., Naser Ahmadi, A., 2009. Solubility of H2S in ionic liquids [bmim][PF 6], [bmim][BF 4], and [bmim][Tf 2 N]. J. Chem. Eng. Data 54 (6), 1844–1849. https://doi.org/10.1021/je8009495.

Hosseinian, A., Ahmadi, S., Mohammadi, R., Monfared, A., Rahmani, Z., 2018. Three-component reaction of amines, epoxides, and carbon dioxide: a straightforward route to organic carbamates. J. CO2 Util. 27, 381–389. https://doi.org/10.1016/j.jcou.2018.08.013.

Huang, Y., Wang, R., 2019. Highly selective separation of H2S and CO2 by core-shell-structure H2S imprinted polymers loaded on polyoxometalate@Zr-based metal-organic framework at ambient temperature. J. Mater. Chem. A Mater. Energy Sustain. https://doi.org/10.1039/C9TA01749F.

Jalili, A.H., Shokouhi, M., Maurer, G., Hosseini-Jenab, M., 2013. Solubility of CO2 and H2S in the ionic liquid 1-ethyl-3-methylimidazolium tris(pentafluoroethyl)trifluorophosphate. J. Chem. Thermodyn. 67, 55–62. https://doi.org/10.1016/J.JCT.2013.07.022.

Kazarian, S.G., Briscoe, B.J., Welton, T., 2000. Combining ionic liquids and supercritical fluids: in situ ATR-IR study of CO2 dissolved in two ionic liquids at high pressures. Chem. Commun. 0, 2047–2048. https://doi.org/10.1039/b005514j.

Kumełan, J., Ä lvaro Pérez-Salado Kamps, A., Tuma, D., Maurer, G., 2006. Solubility of CO 2 in the Ionic Liquids [bmim][CH 3 SO 4] and [bmim][PF 6]. J. Chem. Eng. Data. https://doi.org/10.1021/je060190e.

Lee, H., Ho Cho, M., Sook Lee, B., Palgunadi, J., Kim, H., Sik Kim, H., 2010. Alkylfluoroalkylimidazolium-based ionic liquids as efficient $CO_2$ absorbents. Energy Fuel. 24, 6689–6692. https://doi.org/10.1021/ef101143t.

Lepaumier, H., Picq, D., Carrette, P.-L., 2009. New amines for CO 2Capture. I. Mechanisms of amine degradation in the presence of $CO_2$. Ind. Eng. Chem. Res. 48, 9061–9067. https://doi.org/10.1021/ie900472x.

Liu, X., Huang, Y., Zhao, Y., Gani, R., Zhang, X., Zhang, S., 2016. Ionic liquid design and process simulation for decarbonization of shale gas. Ind. Eng. Chem. Res. 55, 5931–5944.

Ma, T., Wang, J., Du, Z., Abdeltawab, A.A., Al-Enizi, A.M., Chen, X., Yu, G., 2017. A process simulation study of CO2 capture by ionic liquids. Int. J. Greenh. Gas Control 58, 223–231.

Ma, Y., Gao, J., Wang, Y., Hu, J., Cui, P., 2018. Ionic liquid-based CO2 capture in power plants for low carbon emissions. Int. J. Greenh. Gas Control 75, 134–139. https://doi.org/10.1016/J.IJGGC.2018.05.025.

Mattedi, S., Carvalho, P.J., Coutinho, J.A.P., Alvarez, V.H., Iglesias, M., 2011. High pressure CO2 solubility in N-methyl-2-hydroxyethylammonium protic ionic liquids. J. Supercrit. Fluids 56, 224–230. https://doi.org/10.1016/J.SUPFLU.2010.10.043.

McCrellis, C., Taylor, S.F.R., Jacquemin, J., Hardacre, C., 2016. Effect of the presence of MEA on the $CO_2$ capture ability of superbase ionic liquids. J. Chem. Eng. Data 61, 1092–1100. https://doi.org/10.1021/acs.jced.5b00710.

Meindersma, G.W., De Haan, A.B., 2012. Cyano-containing ionic liquids for the extraction of aromatic hydrocarbons from an aromatic/aliphatic mixture. Sci. China Chem. 55, 1488–1499. https://doi.org/10.1007/s11426-012-4630-x.

Mesbah, M., Shahsavari, S., Soroush, E., Rahaei, N., Rezakazemi, M., 2018. Accurate prediction of miscibility of CO 2 and supercritical CO 2 in ionic liquids using machine

learning. J. CO2 Util. 25, 99–107.
Mokhatab, S., 2006. Handbook of Natural Gas Transmission and Processing: Principles and Practices.
Muhammad, A., GadelHak, Y., 2015. Simulation based improvement techniques for acid gases sweetening by chemical absorption: a review. Int. J. Greenh. Gas Control 37, 481–491. https://doi.org/10.1016/J.IJGGC.2015.03.014.
Øi, L.E., Bråthen, T., Berg, C., Brekne, S.K., Flatin, M., Johnsen, R., Moen, I.G., Thomassen, E., 2014. Optimization of configurations for amine based CO2 absorption using aspen HYSYS. Energy Procedia 51, 224–233. https://doi.org/10.1016/J.EGYPRO.2014.07.026.
Raveendran, P., Wallen*, S.L., 2003. Exploring $CO_2$-philicity: effects of stepwise fluorination. J. Phys. Chem. 107, 1473–1477. https://doi.org/10.1021/JP027026S.
Pringle, J.M., Golding, J., Baranyai, K., Forsyth, C.M., Deacon, G.B., Scott, J.L., MacFarlane, D.R., 2003. The effect of anion fluorination in ionic liquids—physical properties of a range of bis(methanesulfonyl)amide salts. New J. Chem. 27, 1504–1510. https://doi.org/10.1039/B304072K.
Privalova, E.I., Mäki-Arvela, P., Murzin, D.Y., Mikkhola, J.-P., 2012. Capturing CO2: conventional versus ionic-liquid based technologies. Russ. Chem. Rev. 81, 435.
Qadeer, K., Qyyum, M.A., Lee, M., 2018. Krill-herd-Based investigation for energy saving opportunities in offshore liquefied natural gas processes. Ind. Eng. Chem. Res. 57, 14162–14172. https://doi.org/10.1021/acs.iecr.8b02616.
Qyyum, Muhammad Abdul, Chaniago, Y.D., Ali, W., Qadeer, K., Lee, M., 2018a. Coal to clean energy: energy-efficient single-loop mixed-refrigerant-based schemes for the liquefaction of synthetic natural gas. J. Clean. Prod. 211, 574–589. https://doi.org/10.1016/j.jclepro.2018.11.233.
Qyyum, M.A., Qadeer, K., Lee, S., Lee, M., 2018b. Innovative propane-nitrogen two-phase expander refrigeration cycle for energy-efficient and low-global warming potential LNG production. Appl. Therm. Eng. 139. https://doi.org/10.1016/j.applthermaleng.2018.04.105.
Qyyum, M.A., Qadeer, K., Minh, L.Q., Haider, J., Lee, M., 2019. Nitrogen self-recuperation expansion-based process for offshore coproduction of liquefied natural gas, liquefied petroleum gas, and pentane plus. Appl. Energy 235, 247–257. https://doi.org/10.1016/J.APENERGY.2018.10.127.
Ramdin, M., Olasagasti, T.Z., Vlugt, T.J.H., de Loos, T.W., 2013. High pressure solubility of CO2 in non-fluorinated phosphonium-based ionic liquids. J. Supercrit. Fluids 82, 41–49. https://doi.org/10.1016/J.SUPFLU.2013.06.004.
Ranke, J., Stolte, S., Störmann, R., Arning, J., Jastorff, B., 2007. Design of sustainable chemical products the example of ionic liquids. Chem. Rev. 107, 2183–2206. https://doi.org/10.1021/cr050942s.
Safavi, M., Ghotbi, C., Taghikhani, V., Jalili, A.H., Mehdizadeh, A., 2013. Study of the solubility of CO2, H2S and their mixture in the ionic liquid 1-octyl-3-methylimidazolium hexafluorophosphate: experimental and modelling. J. Chem. Thermodyn. 65, 220–232. https://doi.org/10.1016/J.JCT.2013.05.038.
Sánchez-Badillo, J., Gallo, M., Alvarado, S., Glossman-Mitnik, D., 2015. Solvation thermodynamic properties of hydrogen sulfide in [$C_4$ mim][$PF_6$], [$C_4$ mim][$BF_4$], and [$C_4$ mim][Cl] ionic liquids, determined by molecular simulations. J. Phys. Chem. B 119, 10727–10737. https://doi.org/10.1021/acs.jpcb.5b06525.
Sarker, N.K., 2016. Theoretical effect of concentration, circulation rate, stages, pressure and temperature of single amine and amine mixture solvents on gas sweetening performance. Egypt. J. Pet. 25, 343–354. https://doi.org/10.1016/J.EJPE.2015.08.004.
Shiflett, M.B., Drew, D.W., Cantini, R.A., Yokozeki, A., 2010. Carbon dioxide capture using ionic liquid 1-butyl-3-methylimidazolium acetate. Energy Fuels 24, 5781–5789.
Song, H.N., Lee, B.-C., Lim, J.S., 2010. Measurement of CO $_2$ solubility in ionic liquids: [BMP][TfO] and [P14,6,6,6][$Tf_2$ N] by measuring bubble-point pressure. J. Chem. Eng. Data 55, 891–896. https://doi.org/10.1021/je9005085.
Stewart, M., Arnold, K., 2011. Gas Sweetening and Processing Field Manual. Gulf Professional Pub.
Taheri, M., Dai, C., Lei, Z., 2018. CO2 capture by methanol, ionic liquid, and their binary mixtures: experiments, modeling, and process simulation. AIChE J. 64, 2168–2180.
Thaim, T.M., 2015. Study on the Foaming Tendency of Ionic Liquids of Different Anion and Nmethyldiethanolamine (MDEA) for the Removal of Carbon Dioxide. UMP.
Tomadakis, M.M., Heck, H.H., Jubran, M.E., Al-Harthi, K., 2011. Pressure-Swing adsorption separation of H2S from CO2 with molecular sieves 4A, 5A, and 13X. Sep. Sci. Technol. 46, 428–433. https://doi.org/10.1080/01496395.2010.520292.
Turton, R., Bailie, R.C., Whiting, W.B., Shaeiwitz, J.A., 2008. Analysis, Synthesis and Design of Chemical Processes. Pearson Education.
Venkatraman, V., Alsberg, B.K., 2017. Predicting CO2 capture of ionic liquids using machine learning. J. CO2 Util. 21, 162–168.
Wang, L., Xu, Y., Li, Z., Wei, Y., Wei, J., 2017. CO2/CH4 and H2S/CO2 Selectivity by Ionic Liquids in Natural Gas Sweetening. Energy Fuels 32, 10–23.
Xiao, D., Hines, L.G., Li, S., Bartsch, R.A., Quitevis, E.L., Russina, O., Triolo, A., 2009. Effect of cation symmetry and alkyl chain length on the structure and intermolecular dynamics of 1,3-dialkylimidazolium bis(trifluoromethanesulfonyl)amide ionic liquids. J. Phys. Chem. B 113, 6426–6433. https://doi.org/10.1021/jp8102595.
Zacchello, B., Oko, E., Wang, M., Aloui, F., 2018. Technical and Economic Analysis of Ionic Liquid-Based Post-Combustion CO2 Capture Process. Springer, Cham, pp. 1393–1411. https://doi.org/10.1007/978-3-319-62572-0_89.
Zeng, S., Zhang, Xiangping, Bai, L., Zhang, Xiaochun, Wang, H., Wang, J., Bao, D., Li, M., Liu, X., Zhang, S., 2017. Ionic-liquid-based CO2 capture systems: structure, interaction and process. Chem. Rev. 117, 9625–9673.
Zubeir, L.F., Lacroix, M.H.M., Meuldijk, J., Kroon, M.C., Kiss, A.A., 2018. Novel pressure and temperature swing processes for CO2 capture using low viscosity ionic liquids. Sep. Purif. Technol. 204, 314–327. https://doi.org/10.1016/J.SEPPUR.2018.04.085.